Electric and magnetic properties of $Al_{65}Cu_{20}(Fe_{1-x}Mn_x)_{15}$ quasi-crystals with x=0.0, 0.2, 0.4 and 0.6

1992 J. Phys.: Condens. Matter 4 735

(http://iopscience.iop.org/0953-8984/4/3/013)

J. Phys.: Condens. Matter 4 (1992) 735–746. Printed in the UK

Electric and magnetic properties of $Al_{65}Cu_{20}(Fe_{1-x}Mn_x)_{15}$ quasi-crystals with $x = 0.0, 0.2, 0.4$ and 0.6

S T Lin†, I M Jiang‡, H Y Cheng†, Y C Chen§ and L S Chou†

† Department of Physics, National Cheng Kung University, Tainan, Taiwan, Republic of China

‡ Department of Physics, National Sun Yet-sen University, Kaohsiung, Taiwan, Republic of China

§ Materials Research Laboratories, Industrial Technology Research Institute, Hsinchu, Taiwan, Republic of China

Received 13 May 1991, in final form 10 September 1991

Abstract. We have prepared the alloys $Al_{65}Cu_{20}(Fe_{1-x}Mn_x)_{15}$ with $x = 0.0, 0.2, 0.4$ and 0.6 by the liquid-quenching method. The alloys with $x = 0.0$ and 0.6 are examined by the transmission electron microscopy. Their electron diffraction patterns demonstrate fivefold, threefold and twofold symmetries of the typical icosahedral symmetries of quasi-crystals. The x-ray diffraction patterns of the samples with $x = 0.0, 0.2, 0.4$ and 0.6 can be indexed with six independent Miller indices of the icosahedral structure of quasi-crystals. Thus we can determine the quasi-lattice constant, which was found to increase with increase in the manganese concentration. The differential thermal analysis measurements show that the icosahedral quasi-crystals $Al_{65}Cu_{20}(Fe_{1-x}Mn_x)_{15}$ with $x = 0.0, 0.2, 0.4$ and 0.6 are in thermodynamically good stable phases. The room-temperature resistivity of the samples are in the range 15.47–30.93 $\mu\Omega$ m, which increases with increase in the manganese concentration. The very high resistivities may be caused by the high density of distorted icosahedral structure defects and the possible s–d resonant scattering. The inversed susceptibility versus temperature for $x = 0.4$ and 0.6 can fit the Curie–Weiss formula. The local magnetic moments are $1.64\mu_B$ and $1.27\mu_B$ per Mn atom for samples with $x = 0.4$ and 0.6, respectively. In contrast the samples with $x = 0.0$ and 0.2 do not display a Curie–Weiss-like behaviour.

1. Introduction

Considerable attention has been paid to icosahedral materials (see, e.g., [1]) since the remarkable discovery of icosahedral symmetry in rapidly quenched $Al_{86}Mn_{14}$ alloy by Shechtman *et al* [2]. The electron diffraction patterns of the icosahedral phase exhibit twofold, threefold and fivefold symmetry of an icosahedra, which is not allowed for usual crystals. Although most icosahedral materials prepared by rapid solidification are metastable phases, yet the newly discovered icosahedral alloys Al–Li–Cu [3], Ga–Mg–Zn [4], Al–Cu–Fe [5, 6] and Al–Cu–Ru [7] are found to form thermodynamically stable phases. In addition, Guryan *et al* [7] and Calvayrac *et al* [8] noticed that the x-ray diffraction peak widths in the icosahedral alloys Al–Cu–Ru and $Al_{65}Cu_{20}Fe_{15}$ are several times narrower than those found in icosahedral Al–Li–Cu [3] and Al–Mn [9], indicating that the phason disorder in $Al_{65}Cu_{20}(Fe,Ru)_{15}$ is suppressed greatly. A lack of phason

0953-8984/92/030735 + 12 $04.50

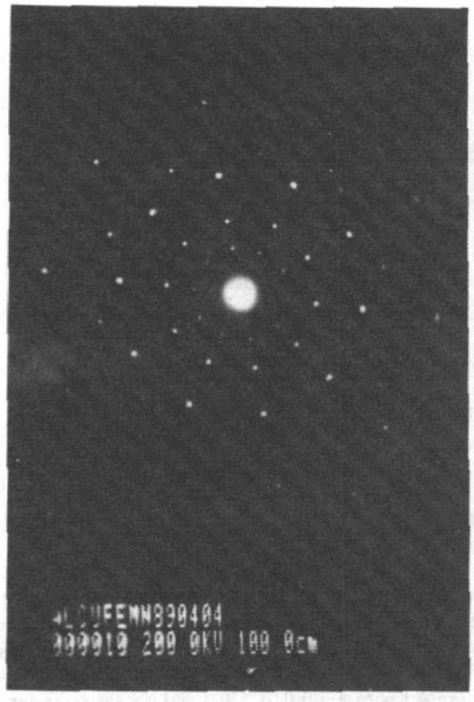

Figure 1. Fivefold electron diffraction pattern of the $Al_{65}Cu_{20}(Fe_{0.4}Mn_{0.6})_{15}$ quasi-crystal.

Figure 2. Threefold electron diffraction pattern of $Al_{65}Cu_{20}(Fe_{0.4}Mn_{0.6})_{15}$.

disorder in these two quasi-crystals would make it more meaningful to study the physical properties of these icosahedral materials.

The resistivities of quasi-crystals are reported to be extremely high. The mean free paths for the electrons in these samples are very short and estimated to be the order of atomic distance with the Drude theory of conduction [10]. The magnetic behaviour is probably influenced by the icosahedral symmetric structures. The typical icosahedral Al–Mn alloys demonstrate a predominant antiferromagnetic Mn–Mn exchange interaction and exhibit spin-glass-like behaviour at low temperatures [11–18]. Another striking feature is that the local magnetic moment associated with Mn atoms has a non-zero value in the quasi-crystalline phase although the crystalline order phase of similar compositions is not magnetic. The quasi-crystal Al–Cu–Fe, however, contains the ferromagnetic element iron; the iron atom does not exhibit any magnetic moment [19]. Thus the effect of icosahedral symmetry is believed to be critical in understanding the physical properties of quasi-crystals. Manganese atoms exhibit an exceptional local magnetic moment in the icosahedral structure. Substituting Mn atoms for Fe atoms may affect the transport and magnetic behaviours of icosahedral $Al_{65}Cu_{20}Fe_{15}$ considerably. In the present work we report our studies on the effects of Mn on the formation, thermal stability, electric properties and magnetic properties of $Al_{65}Cu_{20}(Fe_{1-x}Mn_x)_{15}$ alloys.

2. Experiment

Alloys of the series $Al_{65}Cu_{20}(Fe_{1-x}Mn_x)_{15}$ with $x = 0.0$, 0.2, 0.4, 0.6, 0.8 and 1.0 were prepared by arc melting a mixture of high-purity Al (99.999 wt%), Cu (99.999 wt%),

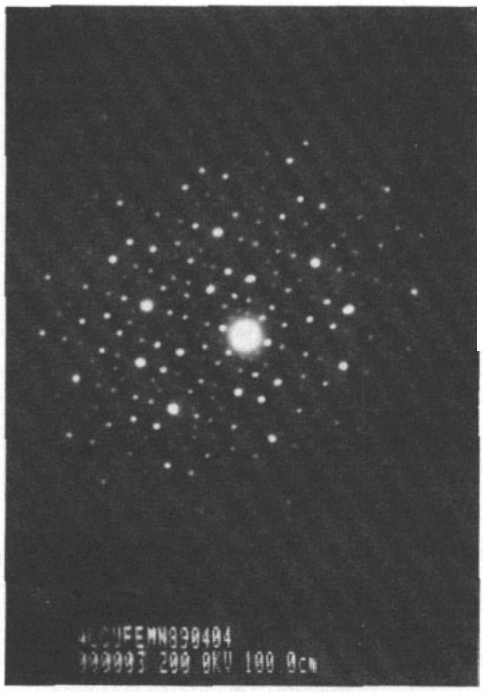

Figure 3. Twofold electron diffraction pattern of $Al_{65}Cu_{20}(Fe_{0.4}Mn_{0.6})_{15}$.

Fe (99.995 wt%) and Mn (99.9 wt%) in a purified argon atmosphere. The compositions are expressed in atomic per cent. The master alloy ingots were melted by induction in a quartz tube. Then the melts were rapidly quenched by ejecting upon a single roller made of copper through an orifice 0.3 mm in diameter with argon. The copper roller (15 cm in diameter) was water cooled and rotated at 6500 rev min^{-1}. The quasi-crystalline samples are in the form of ribbons approximately 20–30 μm in thickness and 1–2 mm in width. The structure was identified using transmission electron microscopy and x-ray powder diffractometry. The thermal stabilities of the samples were studied by means of differential thermal analysis (DTA) measurements. Under an argon atmosphere, measurements were taken with 50 mg pulverized samples at a heating rate of 20 °C min^{-1} from 500 to 1300 °C. Resistivity measurements were taken from 10 K to room temperature using a standard four-point probe technique with Linear Research Inc. LR-400. The DC susceptibility measurements were conducted with a SQUID susceptometer (Quantum Design) in the temperature range from 5 K to room temperature. The applied magnetic field was 10 kG.

3. Results and discussion

In the present work the alloys $Al_{65}Cu_{20}(Fe_{1-x}Mn_x)_{15}$ with $x = 0.0$ and 0.6 have been examined by transmission electron microscopy (TEM). Typical electron diffraction patterns for $Al_{65}Cu_{20}(Fe_{0.4}Mn_{0.6})_{15}$, as shown in figures 1, 2 and 3, reveal fivefold, threefold and twofold symmetrical diffraction spots, respectively, of typical quasi-crystals.

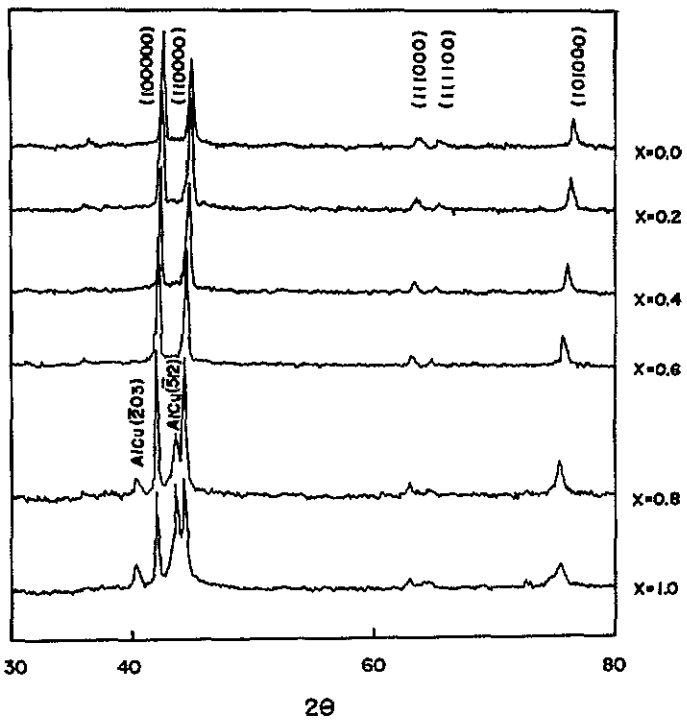

Figure 4. Room-temperature x-ray diffraction patterns for six compositions of $Al_{65}Cu_{20}(Fe_{1-x}Mn_x)_{15}$ with $x = 0.0, 0.2, 0.4, 0.6, 0.8$ and 1.0.

The six compositions of $Al_{65}Cu_{20}(Fe_{1-x}Mn_x)_{15}$ with $x = 0.0, 0.2, 0.4, 0.6, 0.8$ and 1.0 are studied using the room-temperature x-ray powder diffraction method. Figure 4 presents diffraction patterns as a function of diffraction angle for $Al_{65}Cu_{20}(Fe_{1-x}Mn_x)_{15}$ and the diffraction peaks can be indexed by six independent Miller indices following the scheme proposed by Bancel *et al* [20]. We notice that the diffraction patterns of the samples $x = 0.0, 0.2, 0.4$ and 0.6 exhibit a predominantly single icosahedral phase, but the diffraction patterns of samples with $x = 0.8$ and 1.0 show a small fraction of the second phase AlCu. We also notice that the diffraction peaks of icosahedral phase of our samples are located at the almost same positions of the diffraction patterns of quasi-crystals $Al_{65}Cu_{20}TM_{15}$ (TM ≡ transition metals) which have already been identified by Tsai *et al* [6].

The x-ray diffractometry data and the quasi-lattice constant a defined by Elser [21] as the edge length of the rhombohedral cells that make up the three-dimensional Penrose tiling are listed in table 1. The relative intensity of the diffraction peak for all samples decreases in the order (100000) > (110000) > (101000) > (111000) in agreement with the order for the most Al-based quasi-crystals. The lattice constants seem to increase as the concentration of the manganese increases. This may be interpreted in terms of the fact that the atomic radius of manganese is larger than that of iron (Mn, 1.35 Å; Fe, 1.26 Å). The systematic increase may verify the fact that manganese has substituted for iron in the quasi-crystalline structure of $Al_{65}Cu_{20}Fe_{15}$. It should be mentioned that recently Ebalard and Spaepen [22] found that the reciprocal lattice of $Al_{65}Cu_{20}Fe_{15}$ is of the body-centred cubic type rather than of the simple cubic type. Nevetheless, the conclusions drawn above should remain valid.

Table 1. The x-ray diffractometry data of icosahedral $Al_{65}Cu_{20}(Fe_{1-x}Mn_x)_{15}$ with $x = 0.0$, 0.2, 0.4 and 0.6: q_{exp}, I_r and a which are the experimental Bragg vector, relative intensity and quasi-lattice constant, respectively.

	$x = 0.0$		$x = 0.2$		$x = 0.4$		$x = 0.6$	
Reflection	q_{exp}	I_r	q_{exp}	I_r	q_{exp}	I_r	q_{exp}	I_r
(100000)	2.970	100	2.964	100	2.959	100	2.948	100
(110000)	3.127	84	3.124	81	3.116	90	3.106	94
(111000)	4.316	35	4.303	32	4.300	31	4.281	30
(111100)	4.425	33	4.411	29	4.400	28	4.388	27
(101000)	5.063	47	5.049	42	5.038	43	5.022	42
a	4.480 Å		4.504 Å		4.512 Å		4.526 Å	

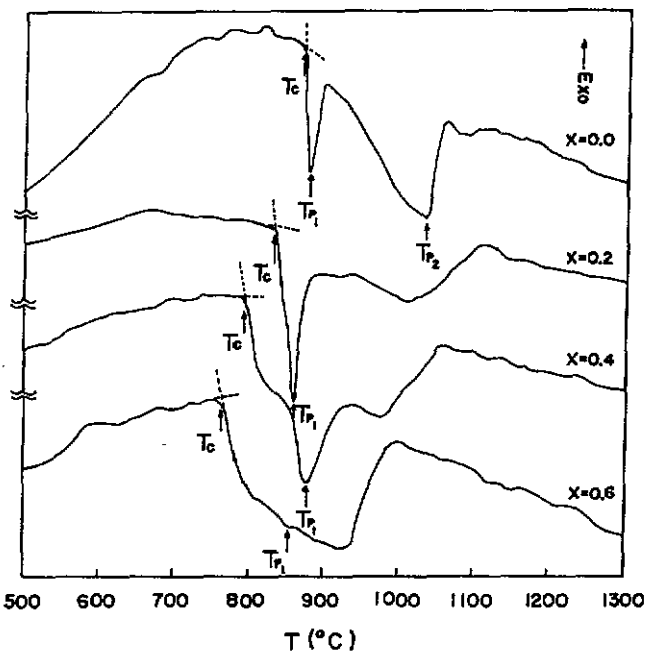

Figure 5. DTA curves of $Al_{65}Cu_{20}(Fe_{1-x}Mn_x)_{15}$ quasi-crystals with $x = 0.0$, 0.2, 0.4 and 0.6.

Figure 5 displays the DTA curves of quasi-crystals $Al_{65}Cu_{20}(Fe_{1-x}Mn_x)_{15}$ with $x = 0.0$, 0.2, 0.4 and 0.6 in the temperature range 500–1300 °C. The DTA curve for sample $x = 0.0$ shows that the heat flow increases as the temperature is increased. Two endothermic peaks are observed. The first appears from 869 °C upwards, as is indicated by T_c in the figure, and the first peak is located at 879 °C, which was identified to be the melting point (T_{p_1}) of the highly thermal stable $Al_{65}Cu_{20}Fe_{15}$ quasi-crystal phase by A. P. Tsai. The second peak at 1034 °C (T_{p_2}) observed in the present experiment deserves further investigation. The samples with $x = 0.2$ and 0.4 behave similarly to the sample with $x = 0.0$. They also exhibit two endothermic peaks, but the two peaks have moved towards

Table 2. T_c, T_{p_1} and T_{p_2} which are the temperatures of onset melting, melting and second peak determined from DTA curves of icosahedral $Al_{65}Cu_{20}(Fe_{1-x}Mn_x)_{15}$ with $x = 0.0, 0.2, 0.4$ and 0.6.

x	T_c (°C)	T_{p_1} (°C)	T_{p_2} (°C)
0.0	869	879	1034
0.2	843	860	1011
0.4	796	878	971
0.6	771	853	—

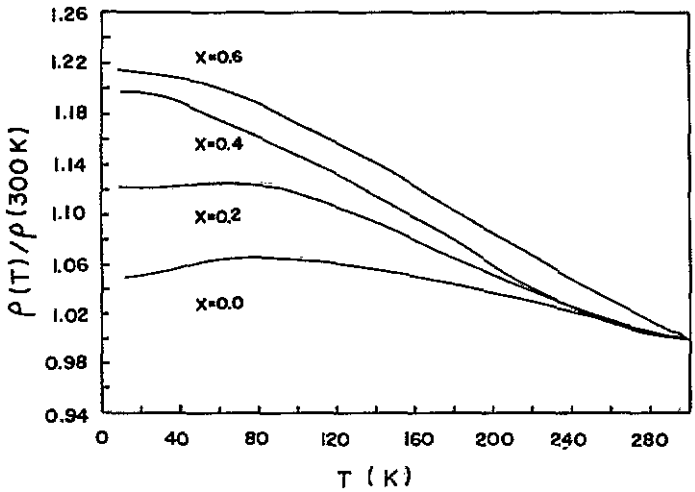

Figure 6. Temperature dependence of the relative resistivity $\rho(T)/\rho(300\,K)$ of $Al_{65}Cu_{20}(Fe_{1-x}Mn_x)_{15}$ quasi-crystals with $x = 0.0, 0.2, 0.4$ and 0.6.

each other. As for the sample with $x = 0.6$, instead of two discrete peaks, there is only one large endothermic peak. The temperatures of onset melting (T_c), melting (T_{p_1}) and second peak (T_{p_2}) of the four samples are listed in table 2. We notice that both the onset melting temperature T_c and the melting temperature T_{p_1} decrease markedly as the manganese concentration is increased. This may be attributed to the fact that manganese atoms of lower melting temperature have replaced iron atoms in the quasi-crystal $Al_{65}Cu_{20}Fe_{15}$ (the melting point of manganese is 1244 ± 3 °C, and that of iron is 1535 ± 3 °C). Since all four samples exhibit neither exothermic nor endothermic peaks before the melting point, the quasi-crystals studied can be said to be in a thermodynamically stable phase.

Figure 6 shows the temperature dependence of the relative resistivity $\rho(T)/\rho(300\,K)$ of $Al_{65}Cu_{20}(Fe_{1-x}Mn_x)_{15}$ quasi-crystals with $x = 0.0$, 0.2, 0.4 and 0.6. All the samples have high resistivities. The high resistivity is ascribed to a very short mean free path, i.e. of the order of interatomic distance, for the conduction electrons in the material. The room-temperature resistivity $\rho(300\,K)$ of the samples are in the range 15.47–30.93 $\mu\Omega$ m, which increases with increase in the manganese concentration. We notice

that the resistivity of all samples increases as the temperature is lowered below room temperature; the temperature coefficient of resistivity, $\alpha = (1/\rho)(d\rho/d\alpha)$, exhibits a negative value. We inspect the resistivities more thoroughly and notice that the resistivity of the sample with $x = 0.0$ exhibits a relative maximum at a temperature of 80 K; then the resistivity decreases as the temperature decreases. The temperature coefficient α, of resistivity is negative in the temperature range 80–300 K and then becomes positive in the temperature range 14–80 K. The samples with $x = 0.2$ and 0.4 exhibit a maximum at 60 K and 21 K, respectively. As for the sample with $x = 0.6$, the resistivity increases as the temperature decreases, and the temperature coefficient is negative in the whole range.

The very high resistivities have been theoretically investigated by Sokoloff [23]. He explores whether the scattering of electrons by the three-dimensional quasi-periodic potential is able to explain the observed high resistivities. Although the quasi-periodic nature of the arrangement of the ions might be responsible for the observed high resistivities, yet the elastic scattering by the potential due to the three-dimensional quasi-periodic lattice does not contribute any resistivity in time-dependent perturbation theory. He further concluded that, although the s–d resonant scattering from the transition metals is stronger, the quasi-crystalline potential cannot account for the observed short mean free paths of real quasi-crystals either. Thus he calculated the incoherent scattering produced by defects and showed that a high density of structural defects due to imperfect Penrose tiling could produce high resistivities and short mean free paths comparable with the experimental results. One may envisage that the unusual icosahedral structures are apt to be distorted and thus very probably cause the high density of structural defects. Furthermore the samples studied in the present work were produced by the non-equilibrium, rapidly quenched method, in which the prevailing structural defects indeed have also made great contributions to the very high resistivities. Since the resistivities of our samples systematically increase with increase in the manganese concentration, we could not exclude the contribution due to the possible s–d resonant scattering mechanism. The manganese atom has fewer 3d electrons than the iron atom, and its half-filled 3d band is closer to the Fermi energy. As the concentration of the manganese atom increases, the number of 3d electrons decreases, and the energy difference between the centre of the 3d band and the Fermi energy decreases, such that the resonant scattering may cause a significant contribution to the resistivity. It should be emphasized that the above explanation may be valid only if the electronic band structure does not change significantly when Fe atoms are replaced by Mn atoms. The temperature variation in the resistivity may be due to the temperature dependence of the pair correlation functions.

Figure 7 shows the magnetization versus the temperature of $Al_{65}Cu_{20}(Fe_{1-x}Mn_x)_{15}$ quasi-crystals with $x = 0.0$, 0.2, 0.4 and 0.6. One notices that the magnetization for samples with $x = 0.0$ and 0.2 shows a large temperature-independent component and exhibits significant magnetization variations only at low temperatures. As for the samples with $x = 0.4$ and 0.6, the temperature-independent component exhibits a great decrease and shows larger magnetization variations at low temperatures. Figure 8 shows the inverse susceptibility versus the temperature of quasi-crystals $Al_{65}Cu_{20}(Fe_{1-x}Mn_x)_{15}$ with $x = 0.0, 0.2, 0.4$ and 0.6. Only the samples with $x = 0.4$ and 0.6 can fit the following Curie–Weiss formula:

$$\chi(T) = \chi_0 + C/(T - \Theta)$$

where C, Θ and χ_0 are the Curie constant, the Curie–Weiss temperature and the temperature-independent susceptibility. The Curie constant can be expressed as

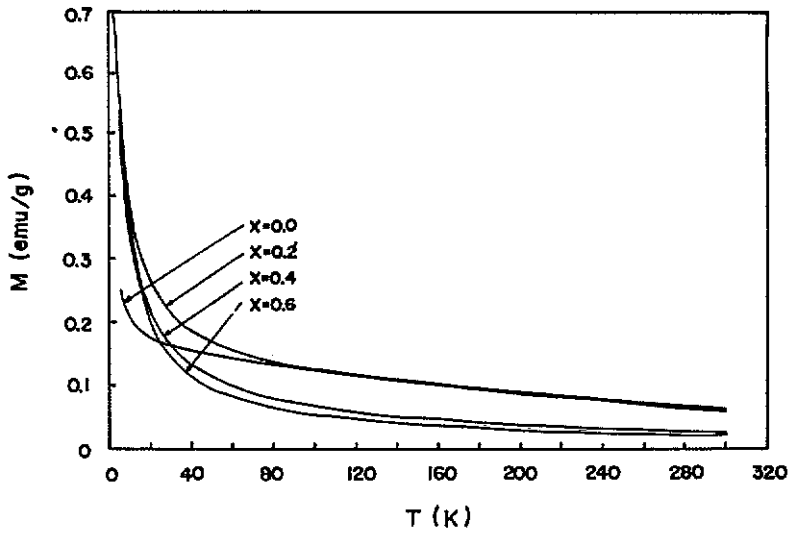

Figure 7. Magnetization versus temperature of $Al_{65}Cu_{20}(Fe_{1-x}Mn_x)_{15}$ quasi-crystals with x = 0.0, 0.2, 0.4 and 0.6.

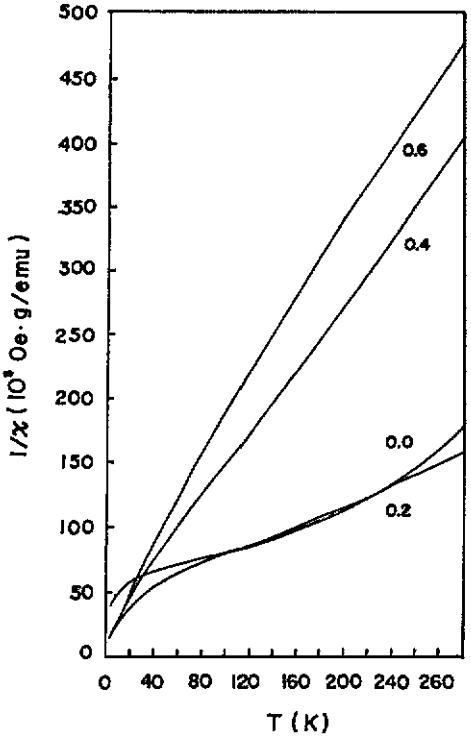

Figure 8. Inverse susceptibility versus temperature of $Al_{65}Cu_{20}(Fe_{1-x}Mn_x)_{15}$ quasi-crystals with x = 0.0, 0.2, 0.4 and 0.6.

Table 3. χ_0, C, Θ and P_{eff} which are the temperature-independent susceptibility, Curie constant, Curie–Weiss temperature and the effective magnetic moment of Mn, respectively.

x	χ_0 (emu g^{-1} Oe^{-1})	C (emu K g^{-1} Oe^{-1})	Θ (K)	P_{eff}(Mn) (μ_B)
0.4	1.3×10^{-6}	5.23×10^{-4}	−5.1	1.64
0.6	6.2×10^{-7}	4.75×10^{-4}	−4.3	1.27

$$C = N_{ion} P_{eff}^2 \mu_B^2 / 3k_B$$

where N_{ion} is the concentration of magnetic ions, P_{eff} is the effective number of magnetic moment in units of the Bohr magneton μ_B and k_B is the Boltzmann constant. As for the samples with $x = 0.0$ and 0.2, the magnetic susceptibility data cannot be fitted by Curie–Weiss law over most of the temperature range measured. This indicates that, for the sample containing no Mn atoms, the magnetic behaviour is more complex, as seen in figure 8.

Matsuo *et al* [19] found that for $Al_{65}Cu_{20}Fe_{15}$, i.e. $x = 0$, the magnetic susceptibility χ increases with increasing temperature T above 100 K and there is a linear relationship between χ and T^2 in the temperature range 150–950 K. In contrast with their observations, we found that χ still decreases with increasing temperature between 100 and 300 K. This is consistent with the observations of Wagner *et al* [24]. In addition, at a temperature of around 770–800 K, Lin and Lin [25] and others [8] have found that a second phase identified as $Al_{14}Fe_3$ is already precipitated out of the $Al_{65}Cu_{20}Fe_{15}$ sample. Therefore, we think that the T^2-dependence of χ observed by Matsuo *et al* may not be the intrinsically magnetic properties of the $Al_{65}Cu_{20}Fe_{15}$ quasi-crystal; the observed difference between the magnetic behaviour of $Al_{65}Cu_{20}Fe_{15}$ observed by Matsuo *et al* and that found by us is possibly due to the difference between the purities and the actual compositions of the samples used. Table 3 gives the determined parameters for the samples with $x = 0.4$ and 0.6. The negative value of Θ indicates a predominantly antiferromagnetic exchange interaction between magnetic ions. The values of P_{eff} per transition-metal atom (i.e. per Mn and Fe) obtained from the Curie constants are 1.04 and 0.98, respectively, for the samples with $x = 0.4$ and 0.6, which virtually remain unchanged. If only the Mn atoms are counted as magnetic atoms, the effective local magnetic moment per Mn will be $1.64\mu_B$ and $1.27\mu_B$ for samples with $x = 0.4$ and 0.6, respectively.

The peculiar local magnetic moment of quasi-crystals has been studied with special local probes, such as nuclear magnetic resonance (NMR) and Mössbauer spectroscopy. Warren *et al* [26] discovered that the intensity of ^{55}Mn NMR line in the icosahedral alloy Al–Mn decreases with increase in the effective local magnetic moment. They suggested that only a fraction of Mn atoms contribute to the bulk paramagnetism since the observed ^{55}Mn NMR line is caused by non-magnetic Mn atoms alone. The Mössbauer measurements have been performed with Al–Mn-based icosahedral alloys in which a fraction of Mn atoms were substituted by Fe atoms. According to the high-field low-temperature ^{57}Fe Mössbauer spectra for the quasi-crystalline $Al_{74}Mn_{20-x}Fe_xSi_6$ ($0.02 \leqslant x \leqslant 7.5$) samples, Eibschütz *et al* [27] found that the hyperfine field is essentially equal to the applied field. This can happen only for Fe atoms with no local magnetic moment. The magnetic susceptibility studies show that these iron atoms in the quasi-crystalline samples possess the same magnetic moment as do the Mn atoms which they replace. Thus the magnetic behaviour of Al–Mn-based icosahedral alloys are usually interpreted with the two-site model that the Mn atoms in the icosahedral alloys occupy

two distinct sites and that the Mn atom carries a significant moment in only one site. Yet through an in-depth analysis of the Mössbauer spectrum of the thermodynamically stable icosahedral $Al_{65}Cu_{20}Fe_{15}$ alloy, Stadnik and co-workers [18, 28] pointed out that two broad structureless lines of the Mössbauer specrum reflect the existence of a multiplicity of Fe sites. They thus argued that the two-site model is inappropriate. Instead, they suggested that the possibility of two classes of Mn atoms (with or without magnetic moment) does not necessarily require the existence of two distinct Mn environments. Rather, such magnetic moment variations could be a consequence of a continuous distribution of interatomic distance, resulting from the intrinsic disorder in icosahedral systems. Thus they suggested that the structure of $Al_{65}Cu_{20}Fe_{15}$ can be thought of in terms of the distorted icosahedral quasi-crystal model.

The formation of the local magnetic moment on Mn atoms in icosahedral alloys has been discussed with the concept of Friedel [29] virtual bound states and the Anderson [30] criterion. Although the Anderson and Friedel theories describe the magnetic behaviour of 3d transition-metal impurities in simple metals, yet this dilute-alloy theory should be taken as a rough approximation. Moruzzi and co-workers [31] have done the calculations using the first-principles total energy band theory for concentrated alloys and showed that transition metals and most probably their alloys as well, favour a magnetic state at large volumes and a non-magnetic state at low volumes. Thus the distance between atoms in the icosahedral quasi-crystal structure is crucial for a site which may or may not carry a magnetic moment.

The local magnetic moments per transition-metal site for the samples with $x = 0.4$ and $x = 0.6$ are not very different from each other. Since the iron level is much deeper in the Fermi surface, one usually deals with the magnetic moment characteristic of manganese atoms and considers that of the iron to be zero. Consequently, the magnetic moment per Mn atom decreases from $1.64\mu_B$ down to $1.27\mu_B$ as the concentration increases from $x = 0.4$ to 0.6. This means that a fraction of the substituting Mn atoms do not have a magnetic moment. The value of the local magnetic moment per Mn site for the sample with $x = 0.4$ is close to the result of Eibschütz *et al*, i.e. $(1.6–1.7)\mu_B$, which is obtained assuming that about 60% Mn sites are magnetic in the quasi-crystalline $Al_{74}Mn_{20}Si_6$ sample. We may expect about 40% of transition-metal sites in $Al_{65}Cu_{20}(Fe_{1-x}Mn_x)_{15}$ quasi-crystals to be able to have a magnetic moment. The experimental results of Mössbauer spectroscopy and NMR reveal that various kinds of Mn site are present in the quasi-crystal. The local magnetic moment of each Mn atom is crucially influenced by its environment, namely its nearest-neighbour atoms. The distorted icosahedral quasi-crystal may form more or less compact local environments for Mn atoms. The local structure may build a larger volume which is favourable to the formation of a magnetic moment, and a smaller volume which is inclined to be non-magnetic. In such a situation, the peculiar local magnetic moment may happen. Also, the imperfections of Penrose tilings, which are affiliated with the distorted icosahedral quasi-crystal, may contribute significantly to the very high resistivities. The novel properties of both the resistivity and the local magnetic moment most probably result from the intrinsic disorder existing in icosahedral quasi-crystals.

4. Conclusion

Prepared $Al_{65}Cu_{20}(Fe_{1-x}Mn_x)_{15}$ with $x = 0.0$, 0.2, 0.4 and 0.6 are found to be thermodynamically stable. All the studied samples manifest a very high resistivity and the

temperature coefficient of resistivity in the samples has a negative value. The incoherent scattering caused by the high density of structural defects may produce high resistivities comparable with the experimental results. Since the resistivities of our samples systematically increase with increase in the manganese concentration, we could not exclude the contribution due to a possible s–d resonant scattering mechanism.

As for the magnetic property of $Al_{65}Cu_{20}(Fe_{1-x}Mn_x)_{15}$ quasi-crystals, the inverse magnetic susceptibility versus temperature can be fitted well using a Curie–Weiss formula. The samples with $x = 0.0$ and 0.2, however, do not display simple Curie–Weiss-like behaviour. If only the Mn atoms are magnetic in $Al_{65}Cu_{20}(Fe_{1-x}Mn_x)_{15}$, the effective local magnetic moments per Mn will be $1.64\mu_B$ and $1.27\mu_B$ for samples with $x = 0.4$ and 0.6, respectively. We estimate that about 40% of the transition metal in the $Al_{65}Cu_{20}(Fe_{1-x}Mn_x)_{15}$ quasi-crystal is capable of having a magnetic moment.

Acknowledgments

The authors are grateful to the National Science Council of the Republic of China for partial support of this work. We also thank Dr H C Yang for magnetic susceptibility measurements and Dr Y D Yao for providing Mn ingots.

References

[1] Steinhardt P J and Ostlund S (ed) 1987 *The Physics of Quasicrystals* (Singapore: World Scientific)
Henley C L 1987 *Comment Condens. Matter Phys.* **13** 59
[2] Shechtman D, Blech I, Gratis D and Cahn J W 1984 *Phys. Rev. Lett.* **53** 1951
[3] Dubost B, Lang J M, Tanaka M, Sainfort P and Audier M 1986 *Nature* **324** 48
Sainfort P and Dubost B 1986 *J. Physique Coll.* **47** C3 321
[4] Ohashi W and Spaepen F 1987 *Nature* **330** 555
[5] Tsai A P, Inoue A and Masumoto T 1987 *Japan. J. Appl. Phys.* **26** L1505
Hiraga K, Zhang B P, Hirabayashi M, Inoue A and Masumoto T 1988 *Japan. J. Appl. Phys.* **27** L951
[6] Tsai A P, Inoue A and Masumoto T 1988 *J. Mater. Sci. Lett.* **7** 322
[7] Guryan C A, Goldman A I, Stephens P W, Hiraga K, Tsai A P, Inoue A and Masumoto T 1989 *Phys. Rev. Lett.* **62** 2409
[8] Calvayrac Y, Quivy A, Bessiere M, Iefebvre S, Cornier-Quiquandon M and Gratias D 1990 *J. Physique* **51** 417
[9] Horn P M, Malzfeldt W, DiVincenzo D P, Toner J and Gambino R 1986 *Phys. Rev. Lett.* **57** 1444
[10] Poon S J, Drehman A J and Lawless K R 1985 *Phys. Rev. Lett.* **55** 2324
Burns M J, Bebrooz A, Yan X, Chaikin P M, Bancel P and Heiney P 1985 *Bull. Am. Phys. Soc.* **31** 268
Pavuna D, Berger C, Cyrot-Lackmann F, Germi P and Pasturel A 1986 *Solid State Commun.* **59** 11
[11] Hauser J J, Chen H S and Waszczak J V 1986 *Phys. Rev.* B **33** 3577
[12] Machado F L A, Clark W G, Azevedo L J, Yang D P, Hines W A, Budnick J I and Quan M X 1987 *Solid State Commun.* **61** 145
[13] Fukamichi K, Goto T, Masumoto T, Sakakibara T, Oguchi M and Todo S 1987 *J. Phys. F: Met. Phys.* **17** 743
[14] Machado F L A, Clark W G, Yang D P, Hines W A, Azevedo L J, Giessen B C and Quan M X 1987 *Solid State Commun.* **61** 691
[15] Lasjaunias J C, Tholence J L, Berger C and Pavuna D 1987 *Solid State Commun.* **64** 425
[16] Machado F L A, Kang W W, Canfield P C, Clark W G, Giessen B C and Quan M X 1988 *Phys. Rev.* B **38** 8088
[17] Laborde O, Frigerio J M, Rivory J, Perez A and Plenet J C 1989 *Solid State Commun.* **71** 711
[18] Stadnik Z M, Stroink G, Ma H and Williams G 1989 *Phys. Rev.* B **39** 9797
[19] Matsuo S, Nakano H, Ishimasa T and Fukano Y 1989 *J. Phys.: Condens. Matter* **1** 6893
[20] Bancel P A, Heiney P A, Stephens P W, Goldman A I and Horn P M 1985 *Phys. Rev. Lett.* **54** 2422

[21] Elser V 1985 *Phys. Rev.* B **32** 4892
[22] Ebalard S and Spaepen F 1989 *J. Mater. Res.* **4** 39
[23] Sokoloff J B 1986 *Phys. Rev. Lett.* **57** 2223; 1987 *Phys. Rev.* B **36** 6361
[24] Wagner J L, Wong K M and Poon S J 1989 *Phys. Rev.* B **39** 8091
[25] Lin C M and Lin S T to be published
[26] Warren W W, Chen H S and Espinosa G P 1986 *Phys. Rev.* B **34** 4902
Warren W W, Chen H S and Hauser J J 1985 *Phys. Rev.* B **32** 7614
[27] Eibschütz M, Lines M E, Chen H S, Waszczak J V, Papaefthymiou G and Frankel R B 1987 *Phys. Rev. Lett.* **59** 244
[28] Stadnik Z M and Stroink G 1988 *Phys. Rev.* B **38** 10 447
[29] Friedel J 1958 *Nuovo Cimento* **2** 287
[30] Anderson P W 1961 *Phys. Rev.* **124** 41
[31] Moruzzi V L, Marcus P M and Pattnaik P C 1988 *Phys. Rev.* B **37** 8003
Moruzzi V L and Marcus P M 1988 *Phys. Rev.* B **38** 1613